Automation of Defect Detection in Digital Radiographic Images

Kimani Njogu
Institute of Nuclear Science and Technology, University of Nairobi, Kenya

David Maina
Institute of Nuclear Science and Technology, University of Nairobi, Kenya

Elijah Mwangi
School of Engineering, University of Nairobi, Kenya

ABSTRACT
Conventionally, it is well-known that diagnosis of defects in an object depends on experience, capability and concentration of the operator. But this process is error prone and liable to subjective considerations such as fatigue, boredom and lapses in operator concentration. This reduces the reliability and consistency of the process thus precluding the undertaking of preventive maintenance with confidence. Also, the process is time consuming and expensive. In this paper, a new automatic defect detection algorithm has been developed in order to identify defects in digital radiographic images. Percolation and Otsu's thresholding and segmentation algorithms have been used and a new procedure for displaying defects on a screen has been developed. Computer simulation based experiments have been used to demonstrate the effectiveness of the proposed algorithm. The performance of the proposed algorithm is found to be better than the existing defect detection algorithms as the results obtained are impressive with respect to the defect detection rate.

Keywords
Binarization, Non-Destructive Testing, Crack detection, Correlation, Percolation.

1. INTRODUCTION
Industrial Non-Destructive Testing (NDT) is a branch of engineering concerned with examining, testing, detecting and evaluating materials for defects or discontinuities that may affect the usefulness or serviceability of an object without causing any physical damage to the material [1]. In the past, humans have been identifying these defects. However, manual detection is a very complicated and a time consuming process. With the advance of science and technology, automated systems have been developed to detect artifacts and defects like cracks [2]. System automation has significantly improved the accuracy of defect detection.

In recent years, numerous algorithms have been proposed and developed in the field of automated systems. For example, a simple and efficient image segmentation algorithm for automated analysis of scanned underground pipe images has been developed by Sinha and Fieguth [3]. However, they did not integrate a way of indicating the severity of the crack. Thiruganam [4] *et al.* proposed a segmentation method on radiographic welds combining global and local thresholding. This gave the defect count and significantly improved the efficiency in terms of computational complexity. Yamaguchi [5] *et al.*, proposed an image processing method based on the percolation model which could be used to detect simple cracks, but because the window for percolation processing was fixed, it could not detect complex cracks accurately. Zhong [6] *et al.*, developed an improvement to Yamaguchi [5] *et al.*, on crack detection algorithm based on the percolation model, which, by reducing the iterations of percolation processing of the whole image, reduces the computation time and improves the efficiency of crack detection. Karsten [7] *et al.*, compared three different crack detection methods of template matching, a sheet filter based on Hessian eigenvalues and percolation thresholding. From these techniques it was found out that it might be relevant to consider template matching when thin cracks are considered. Halfawy and Hengmeechai [8] developed an algorithm for an efficient pattern recognition to support automated detection and classification of pipe defects in images obtained from conventional sewer closed-circuit television (CCTV). The algorithm uses histograms of oriented gradients and support vector machine to identify pipe defects. The method was only applicable on a few defects and CCTV inspections are known to be costly, time consuming, labour intensive and error prone. Finally, Santhi [2] *et al.* has proposed an automation model for crack detection in pavements using edge detection techniques. However, this algorithm has a limitation in that the given image had to be pre-processed to obtain a gray-scale image with square sized dimension before any detection was done. In addition the performance of the algorithm in comparison to other techniques was not investigated.

This paper proposes an automatic defect detection algorithm based on template matching, percolation with a flexible window and Otsu's thresholding techniques. This would eliminate the need of manual operation to identify defects on surfaces. The proposed algorithm is helpful in regard to the reduction of the computational cost and increasing the accuracy of defect detection. In addition, it can detect a large variety of defects like cracks and fractures. Also it has been demonstrated that it is possible to have an algorithm for classification of defects. This algorithm incorporates a way of indicating the severity of the defect by having to set a threshold. If the crack is above a certain threshold, it is severe and it will be indicated by the system. This fulfils the primary goal of NDT for discontinuities in engineering materials, which is to determine whether or not the continuity and homogeneity of a component are adequate for its use.

The rest of this paper is organized as follows: section 2 gives an outline on the theory that is used in developing the proposed algorithm. The theory includes: Otsu's and percolation thresholding methods. Section 3 is a presentation of the proposed method while section 4 gives a presentation of the experimental results obtained using the proposed algorithm. Finally, section 5 gives a conclusion and suggestions on how the work could be extended.

2. THEORETICAL BACKGROUND
2.1 Correlation
In image processing, correlation is a method for establishing the degree of probability that a linear relationship exists between two measured quantities. It involves moving a filter

mask over the image and computing the sum of the products in each location. It is primarily used for locating features in one image that appear in another image.

The correlation of the two functions $f(x, y)$ and a mask $h(x, y)$ is defined as:

$$g(x,y) = \sum_{i=1}^{m} \sum_{j=1}^{n} f(i,j)h(x+i, y+j) \quad (1)$$

where the limits of summation are taken over the region shared by f and h.

In template matching applications, a small reference template with the target defect is found in a large scene image by sliding the template window in a pixel – by – pixel basis. The normalized correlation is then calculated by multiplying the pixels that are overlaid. The maximum values or peaks of the computed correlation values indicate the matches between the template h and the original image f [9].

The term cross correlation is often used in place of correlation to clarify that the images being correlated are different [10]. Normalized Cross Correlation (NCC) has been commonly used as a metric to evaluate the degree of similarity between two images. The main advantage of the normalized cross correlation over the cross correlation is that it is less sensitive to linear changes in the amplitude of illumination in the two compared images. Furthermore, the NCC is confined in the range between -1 and 1. The setting of detection threshold value is much easier than the cross correlation.

The NCC used for finding matches between two images is defined as;

$$\gamma = \frac{\sum_i (x_i - x_m)(y_i - y_m)}{\sqrt{\sum_i (x_i - x_m)^2}\sqrt{\sum_i (y_i - y_m)^2}} \quad (2)$$

where;

x_i and y_i are the intensity values of the pixel in the original and mask images respectively.

x_m and y_m are the mean intensity values of the pixel in the original and mask images respectively.

The NCC is independent of scale changes in the amplitude of f and h. The correlation coefficient has the value $\gamma = 1$ if the two images are absolutely identical while a value of $\gamma = -1$ indicates that the two images have the same shape except that they have the opposite signs. A value of $\gamma = 0$ shows that they are completely uncorrelated [10].

2.2 Image Thresholding

Thresholding is an important technique for image segmentation that tries to identify and extract a target from its background on the basis of the distribution of gray levels or texture in image objects. The threshold of an image is set manually at a specific value or automatically set by an application. Pixels below the set threshold value are converted to black and pixels above the threshold value are converted to white. The thresholding process is sometimes described as separating an image into foreground values and background values and is referred to as binarization [11].

This can be represented as;

$$g(x,y) = \begin{cases} G_a, & f(x,y) \le T \\ G_b, & f(x,y) > T \end{cases} \quad (3)$$

where;

T is the set threshold,

G_a and G_b are the desired gray levels in thresholded image.

Thresholding can be categorized into either global or local thresholding. Global thresholding consists of setting an intensity value (threshold) such that all pixels having intensity value below the threshold belong to one phase and the remainder belong to the other. This is shown in Equation 4. It tries to find a single threshold value for the whole image. Global thresholding is as good as the degree of intensity separation between the two peaks in the image. It is mostly used in images with uniform contrast distribution of background and foreground [11]. This method is very fast in its operation but it tends to produce marginal noise along the page borders of the image. To overcome these complexities, local thresholding techniques have been proposed for image binarization [10].

A global threshold is a value such that:

$$g(x,y) = \begin{cases} 0 \ \ if \ \ f(x,y) \le T) \\ 1 \qquad otherwise \end{cases} \quad (4)$$

where;

T is the threshold value,

$g(x, y)$ is the binarized image and

$f(x, y) \in [0,1]$ be the intensity of a pixel at location (x, y) of the image *f*.

Local thresholding, also called dynamic thresholding, divides the original image into sub-images and then utilizes a different threshold to segment each sub-image. Local thresholding at a pixel level (in comparison with neighbouring pixels) can yield highly superior results compared to global thresholding, particularly for images with varying levels of regional contrast differences. This method is usually able to achieve good results even on severely degraded images, but it is often slow since the computation of image features from the local neighbourhood is to be done for each image pixel [12]. This approach is given in Equation 5, where the image is segmented into three gray regions G_a, G_b and G_c.

$$g(x,y) = \begin{cases} G_a, & 0 \le f(x,y) < T_1 \\ G_b, & T_1 \le f(x,y) < T_2 \\ G_c, & T_2 \le f(x,y) \le G_{max} \end{cases} \quad (5)$$

where G_{max} is the maximum allowable gray level of the image $f(x, y)$.

2.2.1 Otsu's Thresholding

Otsu's method is one of the oldest methods in image segmentation and was proposed by N. Otsu in 1979 [13]. It is a global thresholding selection method and it is popular because of its simplicity and low computational requirements. The basic principle in Otsu's method is to split the image into two classes which are the objects and the background. The automatic threshold is obtained through finding the maximum variance between the two classes. This is done by iterating through all the possible threshold values and calculating a measure of spread for the pixel levels found on each side of the threshold. The aim is to find the threshold value where the sum of foreground and background spreads is at its minimum or looking for the point where the variance is maximum. This is important since well-thresholded classes should be distinct with respect to the intensity values of their pixels [10]. In addition to its optimality, Otsu's method is based entirely on computations performed on the histogram of the image, which is easily obtained.

Consider a digital image of size $M \times N$ pixels with intensity levels {0, 1, 2… L-1}. Let n_i denote the number of pixels with intensity i. The normalized histogram has components $p_i = {n_i}/{MN}$, it then follows that:

$$\sum_{i=0}^{L-1} p_i = 1 \qquad p_i \geq 0 \tag{6}$$

Considering a case of bi-level thresholding, a threshold, $T(k) = k, 0 < k < L - 1$, divides he input image into two classes $C_1$and C_2, where C_1 consists of all the pixels in the image with intensity values in the range $[0, k]$ and C_2 consists of the pixels in the values in the range $[k + 1, L - 1]$ [14]. The probability, $P_1\,(k)$, of a pixel being in class C_1 is:

$$P_1(k) = \sum_{i=0}^{k} p_i \tag{7}$$

Similarly, the probability of class C_2 occurring is:

$$P_2(k) = \sum_{i=k+1}^{L-1} p_i = 1 - P_1(k) \tag{8}$$

The effectiveness of a threshold value at a specific level k is obtained as:

$$\eta = {\sigma_B}^2 / {\sigma_G}^2 \tag{9}$$

where ${\sigma_G}^2$ is the global variance, the intensity variance of all the pixels in the image, given as:

$${\sigma_G}^2 = \sum_{i=0}^{L-1} (i - m_G)^2\, p_i \tag{10}$$

m_G is the global mean denoted as:

$$m_G = \sum_{i=0}^{L-1} i p_i \tag{11}$$

and ${\sigma_B}^2$ is the between-class variance, defined as:

$${\sigma_B}^2 = P_1\,(m_1 - m_G)^2 + P_2(m_2 - m_G)^2 \tag{12}$$

where m_1 and m_2 are the mean intensity values of the pixels assigned to class C_1 and C_2 respectively.

From these computations, the further the two means m_1 and m_2 are from each other, the larger ${\sigma_B}^2$ will be. Therefore, the optimal threshold value, k, should maximize the between-class variance. The above equations can easily be extended for multi-level thresholding of an image [14].

2.2.2 Percolation Thresholding

Percolation is a physical model based on the natural phenomenon of liquid permeation and is effective for describing various phenomena such as electricity conductivity in materials, ferromagnetism and the spread of epidemics [5]. Percolation theory involves the study of discrete objects and their association with each other. This is specifically done by investigating image clusters, their statistics and properties.

Percolation begins at an initial point, and then extends to the surroundings areas according to a probability p, which is a measure of the ease of percolation to the nearest neighbouring region. The point that has the maximum value of p is percolated. Generally, for percolation to occur the critical probability must be higher than 0.5927 otherwise percolation is highly unlikely [15]. This value has been determined empirically. By repeating the percolation process, the region continues to extend until it reaches the border [16]. In image processing based-percolation model, the gray value of each pixel is used to replace the probability p where percolation occurs in the local area. The points with related and similar gray values are percolated and eventually form an image cluster [6].

The basic percolation process consists of four steps.

i) The size of the local window is fixed and the initial pixel at the center of the local window is set. The initial pixel belongs to the percolated region D_p, and the initial threshold is set to the value of the initial pixel brightness.

ii) The threshold T is updated as follows [6]:

$$T = \max\left(\max_{p \in D_p}(V(p))\,, T\right) + \omega \tag{13}$$

where;

$V(p)$ is the brightness of the pixel p,

ω is the acceleration parameter, used to accelerate the percolation.

iii) In D_c (the region consisting of the eight neighbouring pixels of D_p), the pixels whose brightness is below the threshold T are regarded as a part of D_p. Else, the pixel with the lowest brightness in D_c is regarded as a part of D_p.

iv) When D_p reaches the boundary of the local window, the percolation process is terminated. Otherwise, the process returns to the second step. Thus, the final D_p is defined, and a cluster is formed by the percolation process. The focal pixel obtained is evaluated to determine whether it belongs to a crack by characterizing the percolated region (D_p). This is done by using the circularity F_c as a characteristic of D_p as shown;

$$F_c = {4C_{count}} / {(4{C_{max}}^2)} \tag{14}$$

where,

C_{count} is the number of pixels in cluster D_p and,

C_{max} is the diameter of the circumcircle in the percolated cluster that is formed by the proposed scalable window processing.

If the center pixel belongs to crack area, the percolation region grows linearly and the value of F_c is close to zero. Otherwise, the center pixel belongs to background area and the value of F_c is close to 1. Therefore, the value of F_c ranges from 0 to 1, and it can determined whether the center pixel belongs to cracks according to the feature quantity of F_c [6].

Percolation process can be improved by modifying the acceleration parameter, ω. This improved parameter ω' is given as [5];

$$\omega' = F_c . \omega \tag{15}$$

3. PROPOSED METHOD

3.1 Automatic Defect Detection

Thresholding together with correlation were used for automatic defect detection. Otsu's and percolation thresholding techniques were used to eliminate irrelevant information, leaving only the objects of interest in the image. Finally, template matching was used in defect detection as illustrated in Figure 1.

From Figure 1, an image is loaded in MATLAB where it is converted to gray-scale. A binarization process using either Otsu's thresholding or percolation thresholding is then applied to remove unnecessary information in the image. The main process of defect detection using template matching is then performed by using correlation. This involves a direct comparison between the image template and the original image and evaluating the degree to which the two images are similar. This is recorded as the Coefficient of Correlation (CoC), which gives mathematically the degree of correlation between two images. A threshold value is set for CoC and value above the threshold indicates the presence of a defect and it is shown on a screen, otherwise, the defect is not major.

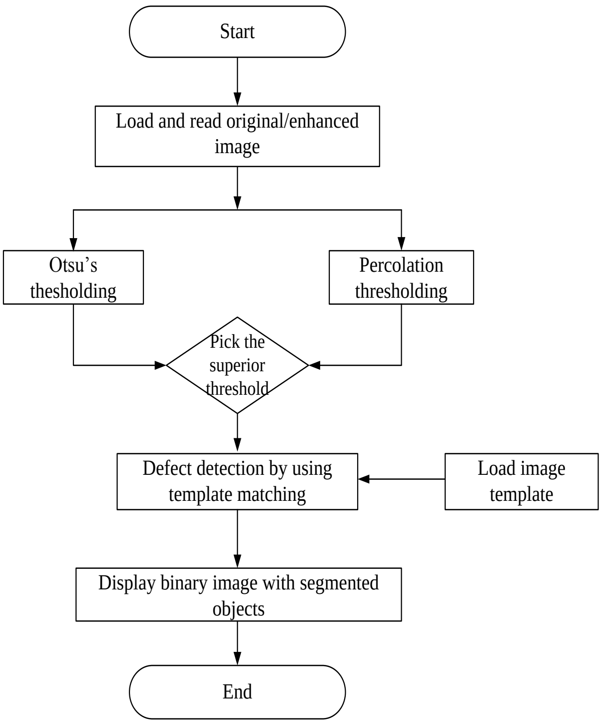

Figure 1: Defect detection flow chart

The method consists of the following procedure;

i) Reading the original X-ray images from the stored database.

ii) Performing either Otsu's or percolation thresholding.

iii) The results obtained by segmentation are used for further higher-level methods of feature extraction. Defects were detected by using template matching.

iv) A threshold value is set for CoC and value above the threshold indicates the presence of a defect, otherwise, the defect is not major.

v) Finally, the presence or absence of a defect is shown on a screen.

4. RESULTS AND DISCUSSION

The results that were obtained from a series of experiments conducted through computer simulations based on MATLAB are presented. A total of twenty nine samples were tested using the proposed methodology. The X-ray images used were obtained from various internet sites. These images have been used by other researches working in the same field [4, 17].

4.1 Image Segmentation

The results in Figure 2 shows the comparison between Otsu's and percolation thresholding. Otsu's thresholding perform clustering-based image thresholding while percolation thresholding describes the behaviour of connected clusters. The identified defects are detected by using connectivity of the surrounding binary images. Figure 2(b) and 2(c) clearly shows the results of Otsu's and percolation thresholded images respectively.

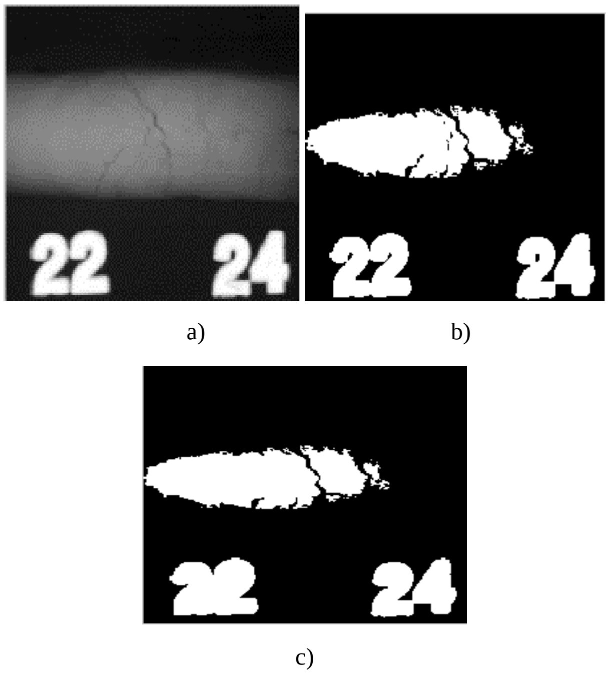

Figure 2: Image segmentation. (a) Input image. (b) Otsu's Thresholding (c) Percolation Thresholding.

4.2 Automatic Crack Detection

Manual inspection of defects have been noted to lack reliability and consistency, precluding the undertaking of preventive maintenance with confidence. Therefore, developing an automatic crack detection and classification method is the inevitable way to solving this problem. This development would be expected to achieve high performance in detection rate, detection accuracy and detection efficiency.

4.2.1 Control experiment

Two images without cracks were used as control experiments. One image as shown in Figure 3(a) was selected and several templates as shown in Figure 3(b), 3(c) and 3(d) were passed over it to try and obtain regions of similar defects by using image correlation. The templates used were from different images and not from the main images. This was done so as to achieve template independence. After passing all the templates over the image, the results in Figure 3(e), 3(f) and

3(g) were obtained. From these results it shows no defect were identified.

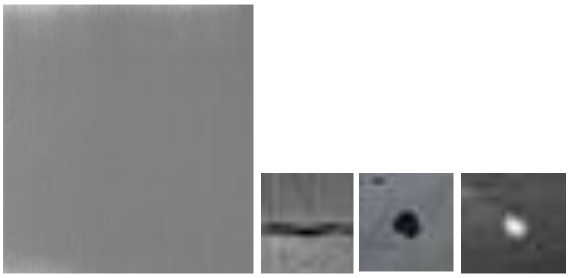

a) b) c) d)

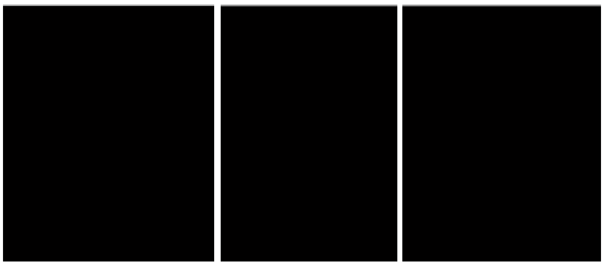

e) f) g)

Figure 3: Control experiment (a) Input image. (b) Horizontal crack template image. (c) Pore1 template image (d) Pore2 template image (e) Horizontal crack result (f) Pore1 template result (g) Pore2 template result

A defect analysis and interpretation algorithm has been developed. This has been implemented by using the Coefficient of Correlation (CoC), which gives the degree of similarity between two images. A series of experiments have shown a threshold of 0.7 to be appropriate. This is higher than the critical threshold required for percolation to occur [15]. Also, a value of 0.7 eliminates unnecessary thresholded information as proved after several experiments. From the proposed algorithm, a value of CoC that is above 0.7 identifies a defect and it is indicates on the screen as shown below.

>>

If maxValue (CoC) is > 0.70, there is a defect

Results

****

First Template a)

There is no defect

****

Second Template b)

There is no defect

****

Third Template c)

There is no defect

>>

4.2.2 Weld Pore

Twelve weld pores spot images were used to test the proposed algorithm. A weld pore image with a defect as shown in Figure 4(a) was selected. Two templates as shown in Figure 4(b) and 4(c) were passed over it in order to identify regions of similar defects by using correlation. The results in Figure 4(d) and 4(e) were obtained indicating the presence of a defect.

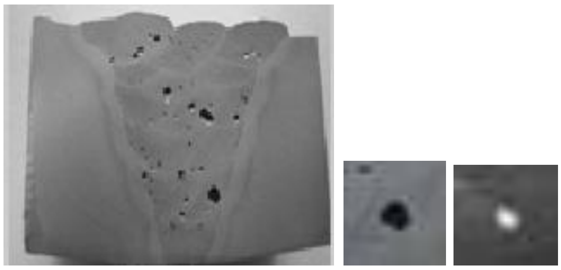

a) b) c)

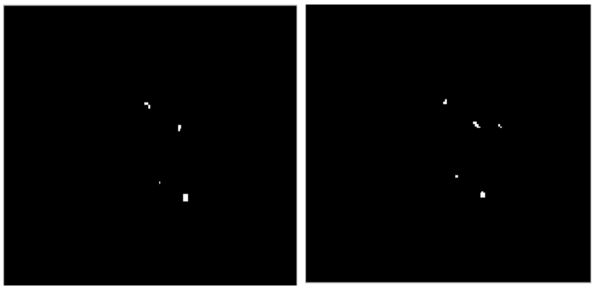

d) e)

Figure 4: Weld pore results. a) Original image b) Pore 1 image c) Pore 2 image d) Pore 1 results e) Pore 2 results

From the algorithm that was developed, the following results were displayed on the screen.

>>

If maxValue (CoC) is > 0.70, there is a defect

Results

****

First Template

There is a defect

****

Second Template

There is a defect

>>

4.2.3 Slag Inclusion

Five weld images with slag inclusions as shown in Figure 5(a) were also used. A template as shown in Figure 5(b) was passed over Figure 5(a) in order to identify regions of similar defects by using correlation. The results in Figure 5(c) were obtained. These results indicates the presence of defects on the original image.

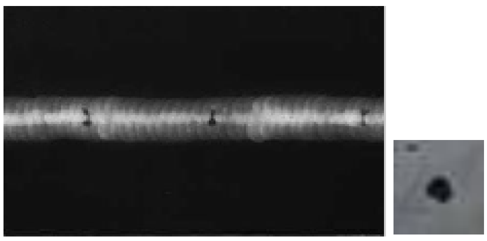

a) b)

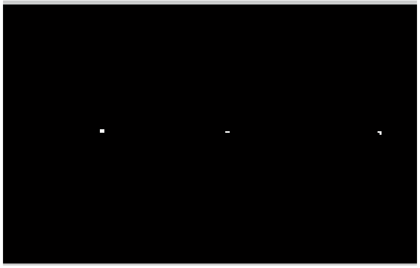

c)

Figure 5: Slag inclusion results. a) Original image b) Slag template image c) Slag template results

From the algorithm that was developed, the following results were displayed on the screen.

>>
If maxValue (CoC) is > 0.70, there is a defect
Results
****
First Template
There is a defect
****
>>

4.2.4 Metal Cracks

Ten metal crack images were used to test the applicability of the proposed algorithm. A metal image with a cracks as shown in Figure 6(a) is discussed. Two templates (with defects) as shown in Figure 6(b) and 6(c) were passed over it in order to identify regions of similar defects by using correlation. The results in Figure 6(d) and 6(e) were obtained indicating the presence of a defect on the original image.

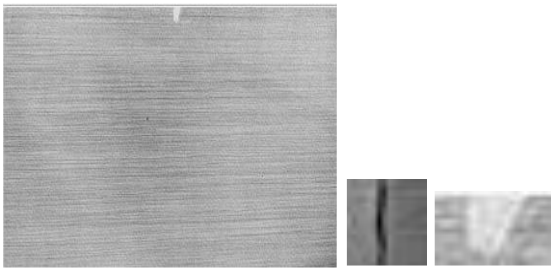

a) b) c)

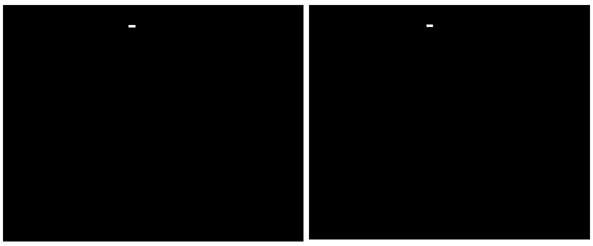

d) e)

Figure 6: Metal crack results. a) Original image b) Vertical template crack c) Pore template image d) Vertical template result e) Pore template result

From the algorithm that was developed, the following results were displayed on the screen.

>>

If maxValue (CoC) is > 0.70, there is a defect

Results

****

First Template

There is a defect

****

Second Template

There is a defect

>>

4.2.5 Template addition

Two templates, Figure 7(b) and 7(c), were added as shown in Figure 7(d) and then passed over Figure 7(a), the original image, to try and identify detect on the original image. The results in Figure 7(e) and 7(g) were obtained indicating the presence of a defect on the original image. Figure 7(f) did not indicate any defect. Figure 7(g) clearly shows that addition of templates can identify defects on an image. A total of ten images were used to test the applicability of this technique.

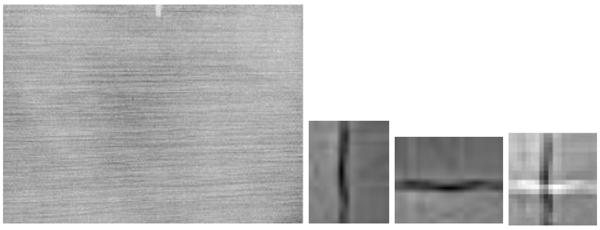

a) b) c) d)

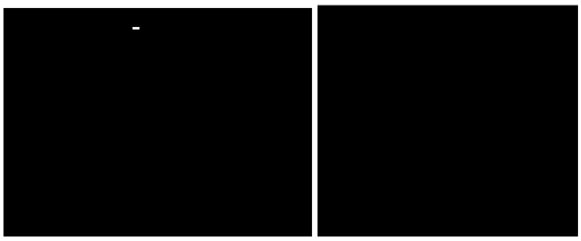

e) f)

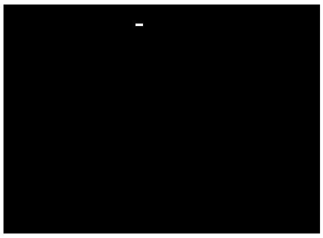

g)

Figure 7: Results of template addition. a) Original image. b) Vertical template crack. c) Horizontal template crack. d) Addition of vertical and horizontal templates. e) Result of template (b). f) Result of template (c). g) Result of addition of template (d).

The following results were displayed on the screen.

If maxValue (CoC) is > 0.70, there is a defect

Results

****

First Template

There is a defect

****

Second Template

There is no defect

****

Third Template

There is a defect

The number of experiments performed and the rate of correct defect detection are summarized in Table 1.

Table 1: Experiments performed and the percentage of correct detection

	Number of images used	**% of correct detection**
Weld spot detection	12	83.3%
Crack detection	10	80.0%
Slag inclusion	5	100%
Template addition	10	90.0%

5. ACKNOWLEDGMENT

The authors would like to thank the International Science Programme, Uppsala University, Sweden, for their research support at the Institute of Nuclear Science and Technology as well as Prof. M. J. Gatari for his suggestions and help. The authors are also grateful to the anonymous reviewers and associate editor for their valuable comments.

6. CONCLUSION

In automatic defect detection, a formulation of a novel image processing method which takes into account the connectivity among neighbourhoods based on either Otsu's thresholding or percolation model were compared. Otsu's techniques proved to be superior through experiments. The results of the automatic defect detection method show that the proposed method produces reliable results which can be used in industries to reduce the effect of errors in detection and to overcome the challenge of always relying on trained operators to identify defects in an image.

There exist much space for future work in order to improve the performance of the proposed algorithm especially on automatic defect detection. For example, to apply the algorithm to a video sequence, instead of static images, by exploiting the motion information and optical flow in tracking and verifying defects over the image sequence.

7. REFERENCES

[1] C. J. Hellier, *Handbook of Non-destructive Evaluation,* McGraw-Hill Companies, Inc., New York, USA, 2003.

[2] B. Santhi, G. Krishnamurthy, S. Siddharth and P. K. Ramakrishnan, "Automatic Detection of Cracks in Pavements using Edge Detection Operator" *Journal of Theoretical and Applied Information Technology*, pp. (199-205), February 2012.

[3] S. K. Sinha and P. W. Fieguth, "Segmentation of Buried Concrete Pipe Images", *Automation in Construction*, 15, (2006), pp. 47 – 57.

[4] M. Thiruganam, S. M. Anouncia and S. Kantipudi, "Automatic Defect Detection and Counting in Radiographic Weldment Images", *International Journal of Computer Applications*, Vol 10– No.2, pp. (1-5), November 2010.

[5] T. Yamaguchi, S. Nakamura, R. Saegusa and S. Hashimoto, "Image-Based Crack Detection for Real Concrete Surfaces", *IEEJ Transactions on Electrical and Electronic Engineering*, 2008; 3: pp. 128–135.

[6] Q. Zhong, L. Lin, Y. Guo and N. Wang, "An Improved Algorithm for Image Crack Detection Based on Percolation Model", *IEEJ Transactions on Electrical and Electronic Engineering*, 2015; 10: pp. 214–221.

[7] E. Karsten, J. Goebbels, D. Meinel, O. Paetsch, S. Prohaska and V. Zobel, "Comparison of Crack Detection Methods for Analyzing Damage Processes in Concrete with Computed Tomography" *International Symposium on Digital Industrial Radiology and Computed Tomography*, Berlin, Germany, pp. (1-8), June 2011.

[8] M. R. Halfawy and J. Hengmeechai "Automated Defect Detection in Sewer Closed Circuit Television Images using Histograms of Oriented Gradients and Support Vector Machine", *Automation in Construction*, 38 pp. (1-13), 2014.

[9] D. M. Tsai, and C. T. Lin, "The evaluation of Normalized Cross Correlations for defect detection", *Pattern Recognition Letters,* vol. 24, pp. 2525-2535, 2003.

[10] R. C. Gonzalez and R. E. Woods, *Digital Image Processing*, Third Edition, Pearson Education, Inc., Upper Saddle River, New Jersey, USA, 2008.

[11] T. S. Romen, S. Roy, O. S. Imocha, T. Sinam and K. Singh "A New Local Adaptive Thresholding Technique in Binarization*" IJCSI International Journal of Computer Science Issues*, Vol. 8, Issue 6, No 2, pp. 271-277, November 2011.

[12] A. R. Weeks, Jr, *Fundamentals of Electronic Image Processing*, Second Edition, SPIE Optical Engineering Press, Bellingham, Washington USA, 1998.

[13] N. Otsu. "A threshold selection method from gray-level histograms". *IEEE Trans. Sys., Man and Cybern,* SMC-9(1): pp. 62-66, January 1979.

[14] P. Liao, T. Chen and P. Chung, "A Fast Algorithm for Multilevel Thresholding", *Journal of Information Science and Engineering*, 17, pp. 713-727, 2001.

[15] M. C. Sukop, G. Van Dijk, E. Perfect and W. P. Van Loon, "Percolation Thresholds in 2-Dimensional Prefractal Models of Porous Media" *Transport in Porous Media*, 48: pp. 187–208, 2002.

[16] T. Yamaguchi, "*A Study on Image Processing Method for Crack Inspection of Real Concrete Surfaces*", Unpublished PhD thesis, Graduate School of Science and Engineering, Waseda University, Tokyo, Japan, 2008.

[17] X-ray film recycling, accessed 01 May 2015 [online] available from <http://www.x-rayfilmrecycling.com/industrial-non-destructive-testing-ndt.html